ENERGY TRANSFER OF PYROPHEOPHORBIDE-a METHYL ESTER IN DIMETHYLFORMAMIDE SOLUTIONS

S. AL-OMARI

Department of Physics, The Hashemite University, Zarqa 13115, Jordan
salomar@hu.edu.jo

Abstract. The photophysical properties of pyropheophorbide- a methyl ester (PPME) were studied in homogeneous organic solvent (dimethylformamide) by means of molecular VIS absorption and fluorescence steady-state and time-resolved spectroscopy. Theoretical calculation on the parameters of homo-Förster resonance energy transfer (FRET) was performed assuming its occurrence between pyropheophorbide-a methyl ester molecules in dimethylformamide solutions. Using the experimental data, the Förster radius for PPME molecules was calculated to be R_0 = 53 Å. The fluorescence quantum yield and lifetime of PPME were found to be 0.21 and 7.3 ns, respectively. The linear differential equations which describe the processes in the Jablonski diagram of PPME were constructed to reveal the kinetics of the transitions.

Key words: Förster resonance energy transfer, donor, acceptor, fluorescence quantum yield, pyropheophorbide-a methyl ester, Jablonski diagram.

INTRODUCTION

Förster resonance energy transfer (FRET) is a distance-dependent interaction in which emission of one fluorophore (donor) is coupled to the absorption of another (acceptor). It takes place mainly because the dipole of the excited donor interacts resonantly with the dipole of the ground state acceptor [50]. The excitation energy of the donor is radiationlessly transferred to a neighbouring acceptor. Consequently, the transferred excitation energy lifts the electron of the acceptor to a higher energy level as a photoexcited electron, while simultaneously the donor returns to its ground state [3].

One of the conditions needed for this mechanism to occur is that the fluorescent emission spectrum of the donor overlaps the absorption spectrum of the acceptor [43]. Furthermore, the transition orientations of the donor dipole and acceptor dipole have to be almost parallel. FRET efficiency of singlet–singlet energy transfer depends on the inverse of the sixth power of the distance between

Received: April 2010;
in final form: August 2010

ROMANIAN J. BIOPHYS., VOL. 20, No. 4, P. 295–314, BUCHAREST, 2010

the fluorophores. This makes possible the measurement of the distance between the interacting fluorophores up to a range from about 10 to 100 Å [12,13]. The energy received by the acceptor is less than that absorbed by the donor due to the Franck-Condon principle [22], the energy difference being spread to the surrounding molecules.

The acceptor can be either fluorescent or nonfluorescent. If the acceptor is fluorescent, the energy transferred to it can be emitted as a characteristic fluorescence emission of the acceptor providing that the donor and acceptor are different fluorophores. The acceptor energy is lost in non-radiative processes when the acceptor is nonfluorescent [41].

It is not necessary that the two fluorophores to be a part of the same molecule. As long as the average intermolecular distances are within 10–100 Å the energy transfer can take place between separated molecules of the same multiplicities [17]. The energy transfer rate is a first order process in the acceptor concentration or donor concentration and the overall energy transfer rate is diffusion-controlled [42].

The distance between the acceptor and donor molecules can be found from the measurements of fluorescence quantum yield or lifetime of the donor. The energy transfer efficiency expresses the overlapping degree between the spectra of the donor emission and the acceptor absorption [9]. This permits the determination of proximity and relative orientation of the interacting fluorophores. Structural information on biological structures was obtained using the calculations of FRET, primarily proteins and other macromolecular assemblies such as ribosomes and nucleosomes [20]. The energy transfer measurements can provide intra- or intermolecular distance data for proteins and their ligands within the range of 10–100 Å. Moreover, FRET can detect changes in distance of 1–2 Å between loci in proteins; hence it is a sensitive tool of the conformational change [21].

Pyropheophorbide a methyl ester (PPME) is an effective second generation photosensitizer of porphyrin derivatives, having a tumorous tissues selective accumulation, small toxicity, and high phototoxicity [1, 2, 11, 19, 29, 30, 34, 44, 46]. The structure of PPME (Fig. 1) is different from that of chlorophyll a by the loss of magnesium from the centre of the molecule, the loss of a carbomethoxy group (–COOCH3) at C10 of the isocyclic ring and the substitution of the phytol group (H39C20) by methyl (CH3) [34, 44]. The great aspect of PPME is its high extinction coefficients around 667 nm and the incorporation of the methyl ester which can increase its lipophilic character [2, 30, 46].

An effective interaction between the covalently linked pheophorbide a moieties was observed for pheophorbide a substituted diaminobuthane (DAB)-dendrimer of a third generation [18]. Along the surface of the dendrimer, the chromophores in the complex undergo homo-Förster energy transfer. These interactions were found to result in a strong reduction of photoactivity of the pheophorbide-a molecules in the complex, especially their singlet oxygen generation and fluorescence quantum yields [18]. The existence of a strong interaction between the identical dye molecules was also observed [51].

The aim of the current work is to perform theoretical calculation on the parameters of homo-FRET process assuming its occurrence between pyropheophorbide a methyl ester molecules in homogeneous organic solvent (dimethylformamide). Jablonski diagram was constructed using the theoretical and experimental data.

MATERIALS AND METHODS

CHEMICALS

Pyropheophorbide a methyl ester (PPME) with a purity of 95% was purchased from Aldrich. Pyropheophorbide-a (PPA) was used as a reference. The used solvent was dimethylformamide (DMF). All chemicals were used as supplied. The structure formulas of PPA and PPME are shown in Fig. 1.

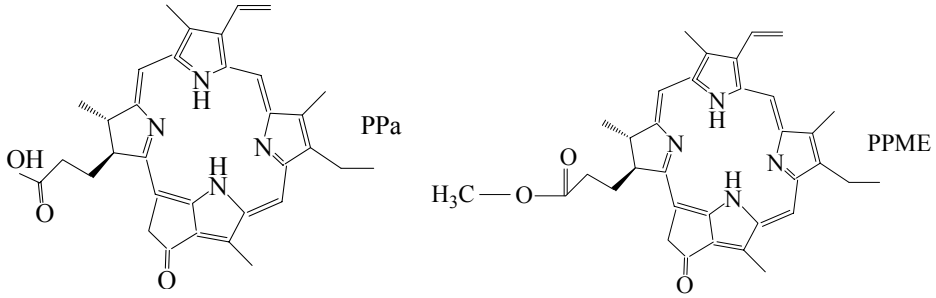

Fig. 1. The structural formulas of pyropheophorbide a methyl ester (PPME) and pyropheophorbide-a (PPA).

ABSORPTION SPECTRA

Ground-state absorption spectra were gathered at room temperature using a commercial spectrophotometer (Shimadzu UV-1700). The wavelength scanning speed was between 10 nm/min ~ and 3000 nm/min; and the wavelength accuracy of ±0.3 nm. The increment of the measurements was 0.1 nm.

FLUORESCENCE SPECTRA

Steady-state fluorescence spectra were taken at 25 °C on an Edinburgh Analytical Instruments Model FS-900 CDT spectrometer. The investigated compounds were measured in 1cm×1cm quartz optical cells using a combination of a cw-Xenon lamp, (XBO150), a polychromator with a cooled photomultiplier (Hamamastu, model IP-28), and an emission monochromator (bandwidth 0.01–9 nm). The slit widths were 5 nm for the excitation and emission light. The signal was acquired for

1 s and the wavelength increment was set to 0.1 nm. The samples were excited at wavelength of 412 nm and their emission spectra were recorded in the spectral range from 300 to 900 nm (2 nm steps) at room temperature.

For the determination of the fluorescence quantum yield (Φ_F), the reference standard of PPA ($\Phi_F = 0.31 \pm 0.02$ in DMF, [2]) was used. To avoid aggregation and reabsorption effects all fluorescence measurements were carried out using solutions with low absorbance ($c < 10^{-6}$ M, optical path length 1 cm). The standard and samples were adjusted to absorbance of 0.2 at 412 nm. Fluorescence quantum yield of PPME (Φ_F^{PPME}) was calculated using the following relationship [2, 23]:

$$\Phi_F^{PPME} = \frac{F^{PPME} A^{PPa} n_{PPME}^2}{F^{PPa} A^{PPME} n_{PPa}^2} \Phi_F^{PPa} \tag{1}$$

where F is the integrated area across the emission band, A is the absorbance at the excitation wavelength, and n is the refractive index of the solvent at 25° which is DMF for the two investigated compounds. The singlet state energy ($E_{1,0}$) was estimated at the point of the normalized absorption and fluorescence spectra [38].

FLUORESCENCE LIFETIME

Fluorescence lifetime measurements were performed at room temperatures on a time-correlated single-photon counting fluorescence spectrometer (Edinburgh Instrument) with CW 450 W xenon arc lamp, nanosecond pulsed flash lamp, 1ns FWHM pulse duration, single photon counting stop photomultiplier, and resolution less than 0.05 nm. Measurements were performed in DMF with excitation wavelength at 412 nm. Data were analyzed by a global iterative program using Marquardt algorithm [28]. Using a single exponential function convoluted by the instrument response function data were both globally and individually analyzed. The goodness of fit was judged using the statistical fit parameter (χ^2) and a random distribution of the residuals.

THEORETICAL METHODS

A donor fluorophore in its excited state can transfer energy by a non-radiative long-range dipole-dipole coupling mechanism to an acceptor fluorophore. The rate of this process was derived by Förster [13, 37]. The electronic energy transfer (EET) rate belongs to the transition from the initial (i) state $D^* + A$, which is described by the two-electron wave function ψ_i to the final (f) state $D + A^*$, that is described by ψ_f [31]:

$$\psi_i = \frac{1}{\sqrt{2}} \left[\psi_D^*(1) \psi_A(2) - \psi_D^*(2) \psi_A(1) \right] \tag{2}$$

$$\psi_f = \frac{1}{\sqrt{2}}\left[\psi_D(1)\psi_A^*(2) - \psi_D(2)\psi_A^*(1)\right] \tag{3}$$

where the asterisk denotes the conjugate of the wave function. The molecular wave function ψ is given by the product of the nuclear χ and electronic Θ wave function according to the Born-Oppenheimer approximation. The element of the interaction matrix (M_{EET}) which represents the coupling between initial and final state is written as

$$M_{EET} = \langle \psi_i | M | \psi_f \rangle \tag{4}$$

$$M = \frac{e^2}{\varepsilon r} \tag{5}$$

where M_{EET} refers to the sum of the two terms of the exchange interaction and columbic interaction, M is the perturbation part of the total Hamiltonian of the system that expresses the repulsion between the two electrons engaged in the energy transfer, ε is the dielectric constant of the solvent, r is the distance between the electrons and e is the electronic charge. It should be emphasized here that energy transfer via Dexter mechanism is acting only between donor and acceptor for short distances range from about 5 to 10 Å [3, 27, 20], therefore it will no further be considered since we are interested in the calculations of FRET which is valid for distances range from about 10–100 Å [3, 12, 17, 22, 41, 43, 50]. By expanding the columbic term we obtain the dipole-dipole term:

$$M_{EET} = \frac{1}{R^3\varepsilon}\left[\boldsymbol{\mu}_A \cdot \boldsymbol{\mu}_D - \frac{3}{R^2}(\boldsymbol{\mu}_A \cdot \mathbf{R})(\boldsymbol{\mu}_D \cdot \mathbf{R})\right]\prod_j \langle \Theta_j^i \mid \Theta_j^f \rangle \tag{6}$$

where, respectively, $\boldsymbol{\mu}_A$ and $\boldsymbol{\mu}_D$ are the transition dipole moments of $A \rightarrow A^*$ and $D \rightarrow D^*$, and $\mathbf{R} = \mathbf{r}_{DA}$ is the centre-to-centre distance between donor and acceptor. The geometrical arrangement of the point dipole-dipole interaction is represented in Fig. 2. Equation (6) can be rearranged by inserting the orientation factor of κ_{DA} [13,27]:

$$M_{EET} = \kappa_{DA}\frac{\boldsymbol{\mu}_A - \boldsymbol{\mu}_D}{R^2\varepsilon}\prod_j \langle \Theta_j^i \mid \Theta_j^f \rangle \tag{7}$$

$$\kappa_{DA} = 2\cos\theta_A \cos\theta_D - \sin\theta_A \sin\theta_D \cos\varphi_T \tag{8}$$

where θ_D and θ_A are the angles between these dipoles and the vector joining the donor and the acceptor, and φ_T stands for the relative orientation of the interacting transition dipole moments (see Fig. 2).

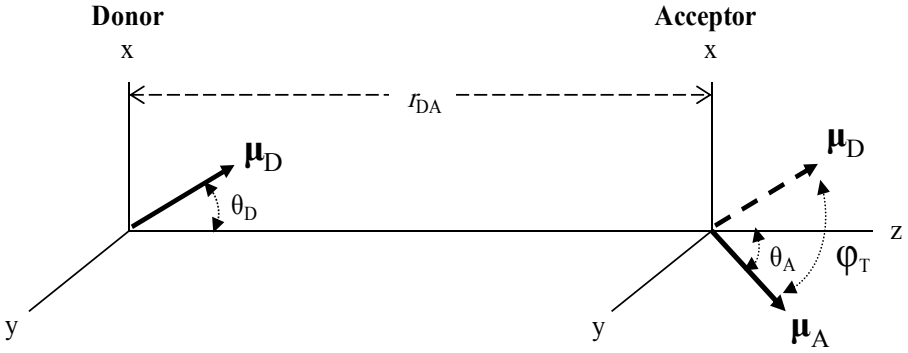

Fig. 2. The graphical representation of the geometrical arrangement of the dipole-dipole interaction. $\boldsymbol{\mu}_A$ and $\boldsymbol{\mu}_D$ are the transition dipole moments of A → A* and D → D*, respectively, r_{DA} is the centre-to-centre distance between donor and acceptor, θ_D and θ_A are the angles between these dipoles and the vector joining the donor and the acceptor, and the φ_T stands for the relative orientation of the interacting transition dipole moments.

The rate constant (k_{eT}) of the energy transfer can be written using Fermi's Golden rule [26]:

$$k_{eT} = \frac{2\pi}{\hbar}\sum_{m,n} P^{\mathrm{i}}\mathbf{M}^2_{EET}\delta\left(E^{\mathrm{i}}_m - E^{\mathrm{f}}_n\right) \tag{9}$$

where P^{i} is the distribution of the initial state, and $E_m{}^{\mathrm{i}}$ and $E_n{}^{\mathrm{f}}$ are, respectively, the energies of the initial (i) and final (f) states and δ – the Kronecker's delta function. By comparing equations (7) and (9), we obtain:

$$k_{\mathrm{eT}} = \frac{2\pi}{\hbar}\left(\frac{\boldsymbol{\mu}_D - \boldsymbol{\mu}_A}{R^3\varepsilon}\kappa_{\mathrm{DA}}\right)^2\left[\sum_{m,n} P^{\mathrm{i}}_m - \left(\prod_j \left\langle \Theta^{\mathrm{i}}_{j,m}\middle|\Theta^{\mathrm{f}}_{j,n}\right\rangle\right)^2 \delta\left(E^{\mathrm{i}}_m - E^{\mathrm{f}}_n\right)\right] \tag{10}$$

The Boltzmann distribution $P_m{}^{\mathrm{i}}$ determines the population of the vibrational states of the excited donor and the ground state acceptor.

RESULTS AND DISCUSSION

ELECTRONIC GROUND-STATE ABSORPTION

The electronic ground-state absorption properties of PPA and PPME were studied in DMF solvent. Their UV-VIS absorption spectra are presented in Fig. 3. The shape of the absorption spectra is similar, but the molar extinction coefficients are higher for PPME, especially at $Q_y(0,0)$ band and Soret band, probably because of the insertion of methyl ester to the macrocyclic structure of PPME molecule.

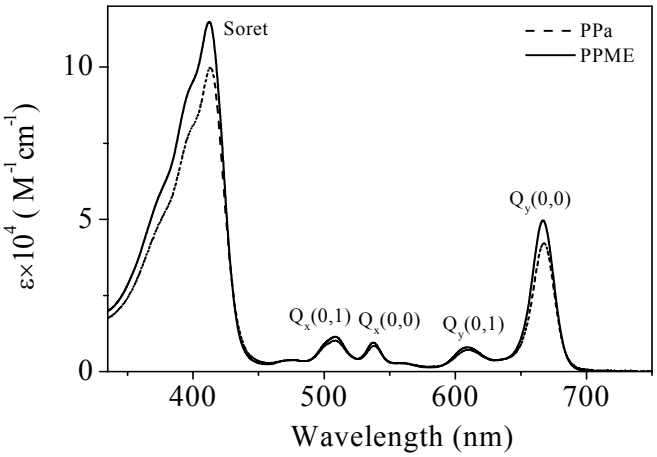

Fig. 3. The VIS absorption spectrum of PPa and PPME in DMF at 25 °C.

The $Q_y(0,0)$ absorption transition at 667 nm of PPa has a molar extinction coefficient of 4.2×10^4 $M^{-1}cm^{-1}$, whereas for PPME at 666 nm this value is 5×10^4 $M^{-1}cm^{-1}$. The Soret band of PPa at 413 nm has a molar extinction coefficient of 9.98×10^4 $M^{-1}cm^{-1}$, whereas this value is 11.47×10^4 $M^{-1}cm^{-1}$ at 412 nm for PPME. The molar extinction coefficients of the rest Q absorption transitions are weak for both molecules and the difference between their molar extinction coefficients is very small. These Q absorption transitions for PPa are $Q_x(0,1)$ at 509 nm, $Q_x(0,0)$ 538 nm, and $Q_y(0,1)$ 610 nm, whereas for PPME they are $Q_x(0,1)$ at 508 nm, $Q_x(0,0)$ at 537 nm, and $Q_y(0,1)$ at 609 nm. The absorption transition bands of PPME exhibit a hypsochromic shift compared to those of PPa. PPME shows higher molar extinction coefficients in the red region of the absorption spectrum which is a demand in photodynamic therapy applications [2, 29 ,30].

The analogues of porphyrins of porphycenes, chlorins, phthalocyanines, purpurins, and naphthalocyanines demonstrated absorption bands peaking at longer wavelengths and showing larger molar extinction coefficients as compared with porphyrins [19, 23, 34, 38, 44]. These spectroscopic features were significant because they guarantee a higher efficiency and probability of light absorption. Actually, the triplet state lifetime, quantum yield of triplet state, and singlet oxygen quantum yield were enhanced for the analogues of porphyrins [19, 23, 34, 38, 44].

FLUORESCENCE AND SINGLET STATE ENERGY

The emission spectra (Fig. 4) were the same for all excitation wavelengths, which shows the existence of only one fluorescing species.

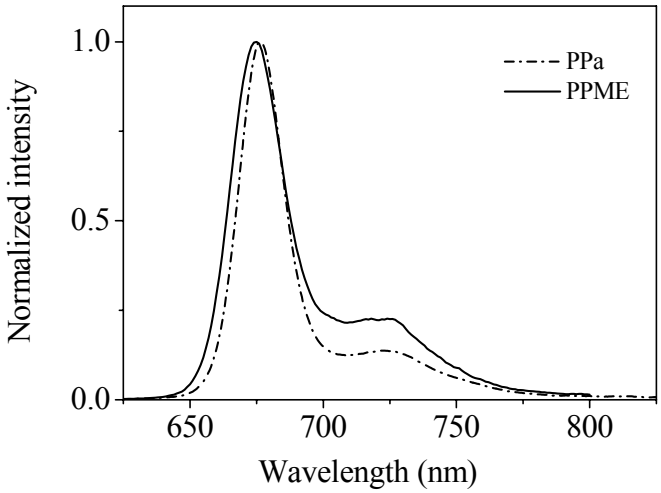

Fig. 4. Fluorescence spectra of pyropheophorbide-a (PPa) and pyropheophorbide-a methyl ester (PPME) in dimethylformamide (DMF) at 25°C. Excitation wavelength (λ_{ex}) = 412 nm. [PPME] = 1.7 μM and [PPa] = 2 μM.

Stokes shift is the difference (in wavelength units) between the positions of the absorption band peak (Fig. 3) and fluorescence emission peak (Fig. 4) [15]. The fluorescence maximum peak in DMF is observed at 675 nm, and therefore PPME exhibits Stokes shift of 9 nm. Stokes shift of PPa is slightly smaller with a value of 8.2 nm. From the intersection of the emission and absorption normalized spectra [38], the singlet state energy $E_{1,0}$ can be evaluated. Calculation gives a value of $E_{1,0}$=1.845 eV which is 0.004 eV blue-shifted compared to that of PPa.

Fluorescence quantum yield of PPME (Φ_F^{PPME}) was determined by the comparison with the reference compound of PPa (Φ_F^{PPA}) according to equation (1). Taking the value of Φ_F^{PPA} as 0.31 ± 0.02 the determined value of Φ_F^{PPME} is 0.21 ± 0.01. A high value of the fluorescence quantum yield is an advantage for a fluorophore in order to serve as a biomarker for tumours. The fluorescence quantum yields of PPa and PPME fall within the range of the porphyrin derivatives being now used in photodynamic therapy [30]. By observing Fig. 3 and Fig. 4 it is found that the absorption and fluorescence spectra are red shifted and structured compared to some porphyrin derivatives [19, 44]. The mirror similarity is not well satisfied.

FLUORESCENCE LIFETIME

The time-resolved measurements of PPa and PPME have shown a single exponential deactivation of the first excited singlet state (Fig. 5). The fit revealed that the lifetime of PPa is τ_F^{PPa} = 6.2 ns and that of PPME is τ_F^{PPME} = 7.3 ns (Table

1). The decay times are relatively high when compared to other porphyrin derivatives [23, 44]. Molecular structures with such properties are known to belong to a planar geometry of the ground and excited states [47]. The higher value of PPME lifetime should result in a decrease of the intersystem crossing quantum yield, and a reduction of the photoinduced singlet oxygen generation [41].

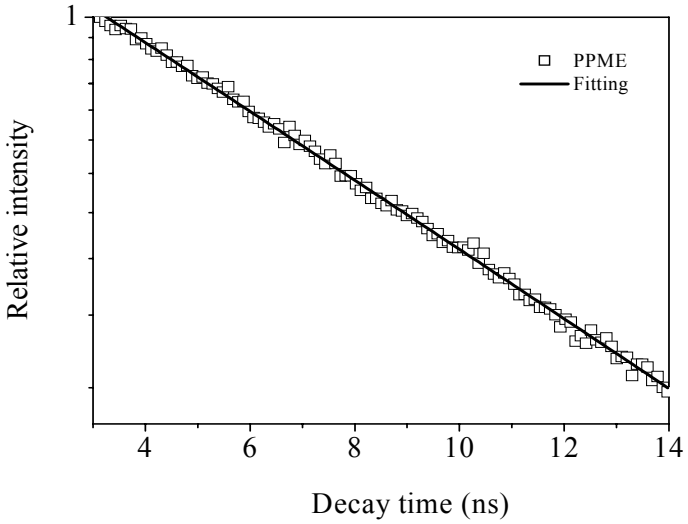

Fig. 5. Fluorescence decay of PPME in DMF monitored at 675 nm. The fit (monoexponential fit) is shown as solid line. Excitation wavelength (λ_{ex}) = 412 nm.

FÖRSTER ENERGY RANSFER

To observe strong nonradiative transitions two conditions have to be fulfilled. First, the molecule must have a large number of vibrational modes in the ground state, which is likely the case for PPME molecular system (see Fig. 3). Second, the coupling of the excited state to the ground vibrational states must be effective [10]. This situation is achieved for specific geometries of the molecules. Prediction of nonradiative relaxation rates would require the information about number and energy of vibrational states. From UV-VIS spectra it is not possible to obtain this knowledge; they are only reflected in the broadening of the different electronic transitions visible in the absorption and fluorescence spectra [45].

Since there is a significant overlap between absorption of the $Q_y(0,0)$ band and fluorescence spectra of PPME, we assume that FRET may occur in such a manner that permits a long-range radiationless intermolecular hopping of energy from an initially excited PPME-donor to other PPME-acceptor. An energy transfer process from PPME as donor is favourable because the energy of the first excited singlet state of PPME is 1.845 eV which is energetically identical to the singlet

state of PPME-acceptor. Moreover, the molar extinction coefficients of PPME-acceptor within the spectral region of the fluorescence spectrum of PPME-donor are large (see Fig. 3 and Fig. 4) [46]. That means that the overlap integral needed for occurring the Förster energy transfer is high as well [6].

One of the most significant parameters when dealing with single dipole-dipole resonance energy transfer is the Förster radius (R_0) at which the energy transfer efficiency from a donor to acceptor is $\Phi_{DA} = 50\%$. In other words, there is an equal probability of resonance energy transfer and radiative emission of a photon [37]. In order to estimate R_0 we used the following formula which is derived from equation (10) [13]:

$$R_0 = \sqrt[6]{\frac{9000(\ln 10)\kappa_{DA}^2 \Phi_D}{128\pi^5 n^4 N_A r_{DA}^6 \tau_D} \int_0^\infty \frac{F_D(\tilde{\nu})\varepsilon_A(\tilde{\nu})}{(\tilde{\nu})^4} d(\tilde{\nu})} \tag{11}$$

where Φ_D is the quantum yield of the PPME-donor in the absence of PPME-acceptor, n = 1.43 is the refractive index of DMF solvent, N_A is Avogadro's number, $F_D(\tilde{\nu})$ is the corrected fluorescence intensity of the donor within wave numbers ranging from $\tilde{\nu}$ to $\tilde{\nu} + d\tilde{\nu}$ with the total intensity normalized to unity, ε_A is the molar extinction coefficient of the acceptor at $\tilde{\nu}$ normalized to peak at unity, and κ_{DA} is a factor describing the relative orientation of the unit vectors which describe the direction of the sensitizers transition dipole moments ($\boldsymbol{\mu}_D$ for the donor and $\boldsymbol{\mu}_A$ for the acceptor, see Fig. 2) in space and their orientation relative to the unit vector separating their centres ($\boldsymbol{r}_{DA}$, see Fig. 2). For the purpose of calculation, κ_{DA}^2 was taken as 2/3 [27]. This average value of the orientation factor is commonly used in solutions with uniform distribution of the transition dipole moments of the interacting molecules [8]. This indicates a randomization of the polarization during energy transfer. In general, the variation of κ_{DA}^2 seems to have no result in serious errors in the calculated distances [8]. Moreover, the flexibility of the fluorophore provides enough dynamic averaging such that the orientation factor does not importantly influence the accuracy of average distance measurements. The uncertainty regarding the orientation factor has nonetheless been a main negative factor in using this technique and several methods were introduced to reduce it [5, 16].

Using equation (11) and the experimental data, the Förster radius for PPME molecules was calculated to be R_0 = 53 Å. This is consistent with those of aromatic compounds where R_0 ranges typically between 10 Å and 100 Å [23, 27, 34]. The significance of Förster radius comes from that the energy transfer measurement is most sensitive to distance variation when donor-acceptor separation is close to their Förster distance [24]. Thus, the approximate dimension of the system to be studied is the most important factor.

An important point regarding the functionality of the drugs (photosensitizers) is the concurrence of the intermolecular or intramolecular energy transfer of the same type of molecules [18, 51]. This will be a problem if the acceptor concentration is high. The critical concentration of PPME-acceptor is [PPME] $= \frac{447}{R_0^3}$ [14, 47, 50], where R_0 has the unit of Å. The intermolecular transfer efficiency at this concentration is 76% [25]. Diffusion can further enhance energy transfer [25, 52]. The concentration of acceptor to avoid intermolecular transfer should be much lower than $\frac{447}{R_0^3}$ [14, 47, 50]. Since the calculated Förster radius of PPME is R_0 = 53 Å, the concentration of the acceptor is [PPME] = 3 mM. With a diffusion coefficient of 3.28×10^{-6} cm^2/s (this value was estimated for PPME using Stokes-Einstein equation [25] at room temperature with PPME radius of 7 Å and DMF viscosity of 0.92 cP), there is about 4% intermolecular energy transfer. Thus, when the acceptor concentration exceeds one hundredth of its critical concentration, a possible intermolecular energy transfer should not be neglected [14].

At Förster distance the summation of the other deactivation efficiencies of the radiative and nonradiative transitions are reduced by 50% [25, 37]. This situation leads necessarily to a serious reduction in the intersystem crossing quantum yield and the singlet oxygen quantum yield. The low singlet oxygen quantum yield reduces the photodynamic activity of the photosensitizer [2, 29, 30]. In order to have further understanding of behaviour of the energy transfer efficiency, it was plotted (Fig. 6) versus the distance between PPME-donor and PPME-acceptor according to equation (12):

$$\Phi_{\mathrm{DA}} = \frac{R_0^6}{R_0^6 + r_{\mathrm{DA}}^6} \tag{12}$$

where r_{DA} is the distance separating the centres of the transition dipoles of donor-acceptor pair (see Fig. 2).

As seen, the efficiency decreases with increasing the distance and practically it is negligible at a distance larger than r_{DA} = 160 Å. Therefore, to avoid the dipole-dipole interaction the distance between the molecules should be larger than this value. Moreover, at the centre-to-centre distance between donor and acceptor (r_{DA}) when it equals to the radius of PPME molecule (the radius of PPME is 7 Å, this radius was estimated using Arguslab program package [4]) the efficiency of energy transfer becomes unity (see Fig. 6). Practically, there is no fluorescence or other deactivation process other than the energy transfer. However, this is not the case, since as the distance between the fluorophores decreases, short-range interactions such as electron exchange interaction and penetration effects may no longer be

negligible [3, 10, 20, 26, 27, 43]. Such proximity may be faced *in vivo*, where the sensitizers trend to accumulate in a definite tissue. Therefore, electron transfer mechanism or energy transfer should be taken into consideration for this situation.

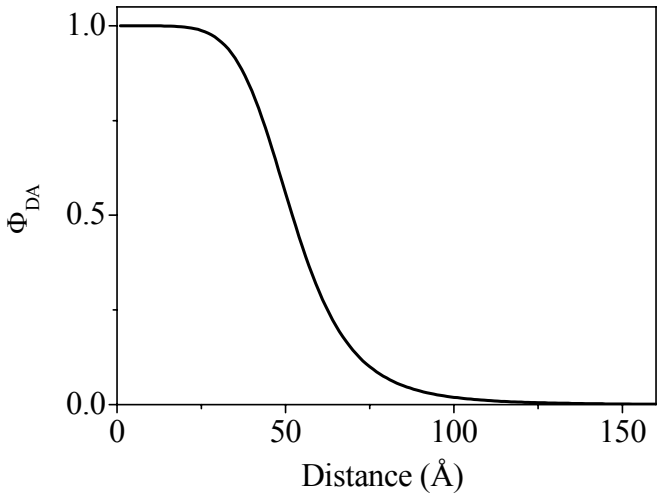

Fig. 6. The distance (r_{DA}) dependence of the energy transfer efficiency (Φ_{DA}) of PPME in DMF.

Because of the sixth power dependence on the distance between donor and acceptor, the variation in Φ_{DA} (Equation (12)) has an inflexion point around $r_{DA} = R_0 = 53$ Å, as shown in Fig. 6. For $r_{DA} < 53$ Å/2, the energy transfer efficiency is close to unity, and for $r_{DA} > 2\times53$ Å, it approaches zero; therefore the distance between donor and acceptor should be in the following range 0.5×53 Å $< r_{DA} < 1.5\times53$ Å. Based on this, the resonance energy transfer can be used as a sensitive spectroscopic ruler for long range distance determination in biology [32, 33]. Furthermore, small changes in R_0 (1–2 Å) and small orientation changes between the donor and acceptor fluorophores can significantly influence the efficiency of FRET, making very small changes in structure easily observable. However, the limitation is that FRET is effective only between 10–100 Å, and the two fluorophores must be maintained in close proximity.

The estimation of the energy transfer efficiency allows us to determine the lifetime of the donor in the presence of the acceptor (τ_{DA}) by using the formula:

$$\frac{\tau_{DA}}{\tau_D} = 1 - \Phi_{DA} \tag{13}$$

where τ_D is the fluorescence lifetime of PPME-donor in the absence of the acceptor.

Fig. 7 shows the calculated value of τ_{DA} as a function of the distance between the PMEE-donor and PPME-acceptor. As seen, at a contact distance of r_{DA} = 7 Å the fluorescence lifetime becomes $\tau_{DA} = 4 \times 10^{-14}$ s (Table 1). That means that there is an efficient energy transfer and most donor molecules are sharing in this mechanism. However, as already mentioned, it should be taken into consideration that Förster theory is not valid when the donor and acceptor are very close since multipole and electron exchange interactions can result in energy transfer as well. Thus, the donor fluorescence will be completely quenched.

Starting from a distance of about r_{DA} = 80 Å (Table 1 and Fig. 7), the ratio between the lifetime in the presence and absence of the energy transfer (τ_{DA}/τ_D) is about 0.90, which indicates that the acceptor starts to have a minor effect on the donor properties. This effect vanishes completely at 160 Å (see Table 1, Fig. 6, and Fig. 7).

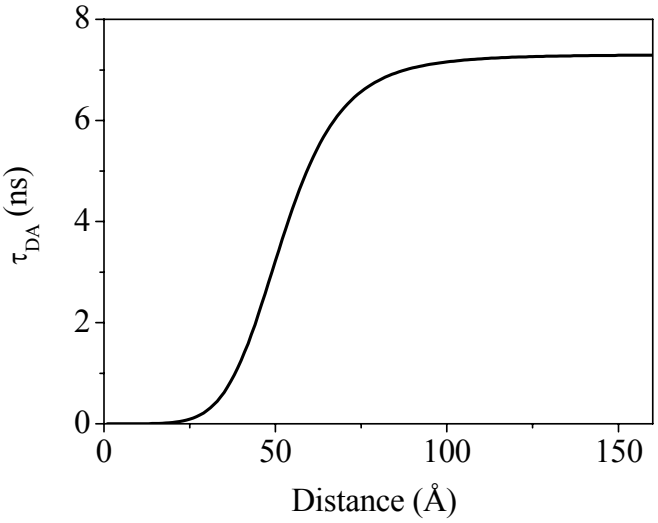

Fig. 7. The lifetime of PPME-donor in the presence of the acceptor (τ_{DA}) as a function of the donor-acceptor pair distance (r_{DA}).

The theory developed by Förster allows the estimation of energy transfer rate (k_{eT}) based on equation (10) according to the formula [42]:

$$k_{eT} = \frac{9000(\ln 10)\kappa_{DA}^2 \Phi_D}{128\pi^5 n^4 N_A r_{DA}^6 \tau_D} \int_0^\infty \frac{F_D(\tilde{\nu})\varepsilon_A(\tilde{\nu})}{(\tilde{\nu})^4} d(\tilde{\nu}) \tag{14}$$

The energy transfer rate was plotted against the distance of donor acceptor pair as depicted in Fig. 8.

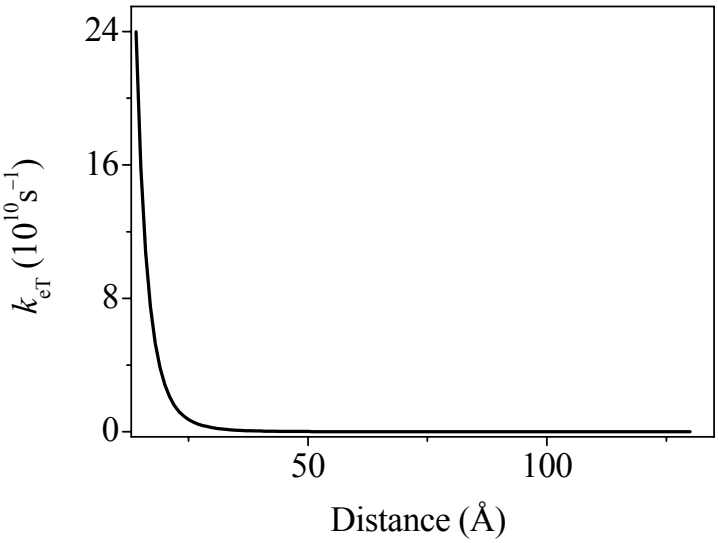

Fig. 8. The energy transfer rate from PPME-donor to PPME-acceptor (k_{eT}) as a function of the donor-acceptor pair distance (r_{DA}).

At a distance of 20 Å the rate of energy transfer is $k_{eT}^{20\text{Å}}$=2.8×10^{10} s^{-1} (Table 1) which is three orders of magnitude higher when compared with the other deactivation rates of fluorescence rate constant of k_F = 3.17×10^7 s^{-1}, internal conversion (IC) rate constant of k_{IC} = 7.5×10^7 s^{-1}, and intersystem crossing (ISC) quantum yield of k_{ISC} = 3.3×10^7 s^{-1}. These rate constants were calculated by dividing the corresponding quantum yield by fluorescence lifetime [35, 49]. Therefore, the fluorescence quenching by energy transfer is very efficient at this distance. This means that the excitation remains approximately $\frac{1}{k_{eT}^{20\text{Å}}}$ = 36 ps only at the initially excited molecule before hopping to another PPME molecule. At a distance of 80 Å the energy transfer rate is k_{eT} = 7×10^6 s^{-1} (Table 1) which is for instance 2% compared to that of the intersystem crossing. However, even such small ratio is not desirable since it contributes in reducing the singlet oxygen of the sensitizer [18, 41, 51]. A dramatic decrease in the energy transfer takes place when the distance between the acceptor and donor changes from 20 Å to 80 Å which is rationalized in terms of the fact that the Förster transfer rate decreases with $\frac{1}{r^6}$ (see equation (14)). That assures that the energy transfer is a sensitive tool that can be used to estimate the distance between the donor and acceptor.

Table 1

Photophysical parameters of pyropheophorbide-a methyl ester (PPME) in dimethylformamide

R_0, Å	53
Φ_D	0.21
$\Phi_{DA}^{20\text{Å}}$	0.997
$\Phi_{DA}^{80\text{Å}}$	0.07
$\Phi_{DA}^{160\text{Å}}$	0.001
τ_D, s	7.3×10^{-9}
$\tau_{DA}^{7\text{Å}}$ (s)	4×10^{-14}
$\tau_{DA}^{20\text{Å}}$ (s)	2×10^{-11}
$\tau_{DA}^{80\text{Å}}$ (s)	6.8×10^{-9}
$\tau_{DA}^{160\text{Å}}$ (s)	7.3×10^{-9}
$k_{eT}^{20\text{Å}}$ (s^{-1})	2.8×10^{10}
$k_{eT}^{80\text{Å}}$ (s^{-1})	7×10^{6}
$k_{eT}^{160\text{Å}}$ (s^{-1})	3×10^{4}

R_0 is Förster radius, Φ_D is the fluorescence quantum yield of PPME, Φ_{DA} is the energy transfer efficiency from PPME-donor to PPME-acceptor, τ_D is the fluorescence lifetime of PPME, τ_{DA} is the fluorescence lifetime of PPME-donor in the presence of the PPME-acceptor, and k_{eT} is the energy transfer rate from PPME-donor to PPME-acceptor.

JABLONSKI DIAGRAM IN THE PRESENCE OF FRET

Using the experimentally determined and/or computed parameters of PPME and the equations (15) to (21), the scheme of the energy levels (Jablonski diagram) [33, 39] of the molecular oxygen (O_2) and PPME molecular system dissolved in DMF as well as the transitions between them have been represented and are shown in Fig. 9. Since molecular oxygen deactivates the triplet state of the photosensitizer to generate singlet oxygen [2, 29, 34, 41], it is necessary to insert it in the Jablonski diagram. Then, linear differential equations were set up and solved to obtain the time-dependent population of the ground and excited states. Hence, an expression for the theoretical time-dependent fluorescence $I_{cal}(t)$ was formulated.

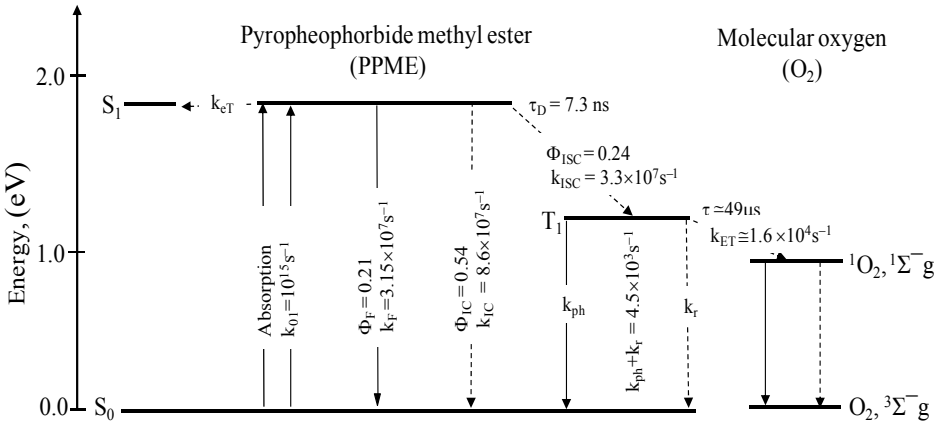

Fig. 9. The scheme of energy levels (Jablonski diagram) of PPME molecular system dissolved in DMF and molecular oxygen (O_2) with the possible transitions between them.

The mathematical modelling of PPME-electronic system is expected to provide an enhanced understanding of the transfer processes from an initially excited PPME-donor to PPME-acceptor and the subsequent nonradiative and radiative processes. The linear differential equations which describe the processes in the Jablonski diagram of PPME shown in Fig. 9 under the condition that k_{01} is zero at $t = 0$, after finishing the pumping, is given by:

$$\frac{\partial}{\partial t}\begin{pmatrix}[S_0]\\ [S_1]\\ [T_1]\end{pmatrix}=\begin{pmatrix}0 & k_F+k_{IC} & k_{ph}+k_r\\ 0 & -(k_{eT}+k_F+k_{IC}+k_{ISC}) & 0\\ 0 & k_{ISC} & -(k_{ET}+k_r+k_{ph})\end{pmatrix}\begin{pmatrix}[S_0]\\ [S_1]\\ [T_1]\end{pmatrix} \tag{15}$$

where, $[S_1]$ is the concentration of PPME molecules in its first excited state, $[S_0]$ is the concentration of molecules in the ground state, $[T_1]$ is the concentration of molecules in the triplet state, k_{ET} is the rate of energy transfer from the triplet state of photosensitizer to the molecular oxygen by Dexter mechanism of electron exchange [41], k_{ph} is the phosphorescence rate constant of the transition $T_1 \rightarrow S_0$, k_r stands for the radiationless rate of the transition $T_1 \rightarrow S_0$ (Fig. 9), k_{eT} is the constant rate for FRET, k_{IC} is the constant rate for the internal conversion, and k_{ISC} is the constant rate for the inter-crossing system process.

The total concentration $[N_T]$ is represented by $[S_1]+[S_0]+[T_1]$ [39, 40].

Equation (15) describes the time-dependent concentrations of the three-level (S_0, S_1, and T_1) system of PPME. The rate equations in equation (15) are linear differential equations of first order of the form $\frac{\mathrm{d}x}{\mathrm{d}t}+g(t)\,x=h(t)$ which have the solution $x\mathrm{e}^{\int g(t)\mathrm{d}t}=\int h(t)\mathrm{e}^{\int g(t)\mathrm{d}t}\mathrm{d}t+c$ [36], where c is a constant. Therefore, solution of the differential equations of the three levels as function of time can be

exactly solved in an algebraic closed form under the condition that the first triplet state and the ground state are not populated at $t = 0$ before starting deactivation of S_1 state [39, 40]. Thus, we can write:

$$[S_1] = [S_1^*]\, \mathrm{e}^{\frac{-t}{\tau_{DA}}} \tag{16}$$

where, τ_{DA} is the donor lifetime in the presence of the acceptor [48]. It is clear that the deactivation of the first excited state according to equation (16) is a monoexponential.

$$[T_1] = [S_1^*] \frac{k_{ISC}\, \tau_{DA}\, \tau_T}{\tau_{DA} - \tau_T} \left(\mathrm{e}^{\frac{-t}{\tau_{DA}}} - \mathrm{e}^{\frac{-t}{\tau_T}} \right) \tag{17}$$

$$[S_0] = \tau_{DA} [S_1^*] (k_F + k_{IC}) \left(1 - \mathrm{e}^{\frac{t}{\tau_{DA}}} \right) + \frac{\tau_{DA}\, \tau_T [S_1^*]\, k_{ISC}}{\tau_{DA} - \tau_T} (k_{ph} + k_r) \left(\tau_T\, \mathrm{e}^{\frac{-t}{\tau_T}} - \tau_{DA}\, \mathrm{e}^{\frac{-t}{\tau_{DA}}} \right) \tag{18}$$

where $[S_1^*]$ is the concentration of the first excited state at $t = 0$.

$$\tau_{DA} = \frac{1}{k_{eT} + k_F + k_{IC} + k_{ISC}} \tag{19}$$

The triplet lifetime is denoted by τ_T and is represented by:

$$\tau_T = \frac{1}{k_{ET} + k_r + k_{ph}} \tag{20}$$

The theoretical fluorescence intensity $I_{cal}(t)$ that is emitted from the excited molecules is proportional to the product of the time-dependent population of the S_1 state and the radiative rate constant. Thus, we can write:

$$I_{cal}(t) = k_F [S_1^*] \mathrm{e}^{\frac{-t}{\tau_{DA}}}. \tag{21}$$

It is important to stress that from equation (21) the time-dependence of the fluorescence decay of PPME is monoexponential. The experimental data confirm this, as the fit in Fig. 5 is monoexponential.

CONCLUSIONS

The above presented investigations have shown that an energy transfer process from PPME as donor to PPME as acceptor is favourable because the energy of first excited singlet state of PPME is 1.845 eV which is energetically identical to that of PPME-acceptor. Moreover, the molar extinction coefficients of PPME-acceptor within the spectral region of the fluorescence spectrum of PPME-

donor are large. Thus, the overlap integral needed for taking place the Förster energy transfer is high as well. Consequently, an intermolecular dipole-dipole Förster energy transfer can appear, and a hop from an initially excited of PPME-donor can take place when they are close to each other. Using VIS absorption and fluorescence spectral experimental data, the Förster radius for PPME molecules was calculated to be $R_0 = 53$ Å. It was found that at an acceptor concentration of [PPME] = 3mM, with a diffusion coefficient of 3.28×10^{-6} cm^2/s, there is about 4% intermolecular energy transfer. Therefore, when the critical concentration of an acceptor exceeds one hundredth of its critical concentration, a possible intermolecular energy transfer should not be neglected, which will be on the account of the other deactivation processes *via* fluorescence, internal conversion, and intersystem crossing. The time-dependent concentrations of the ground and excited states of PPME can be revealed by constructing a set of linear differential equations which describe the processes in the Jablonski diagram.

Acknowledgments. Financial support by The Deanship of Research and Graduate Studies of The Hashemite University is acknowledged. Thanks to Dr. N. Saleh and Mr. K. Aqel for technical assistance.

REFERENCES

1. ALLISON, R.R., G.H. DOWNIE, R. CUENCA, X.H. HU, C.J.H. CHILDS, C.H. SIBATA, Photosensitizers in clinical PDT, *Photodiag. Photodyn. Ther.,* 2004, **1**, 27–42.
2. Al-OMARI, S., A. ALI, Photodynamic activity of pyropheophorbide methyl ester and pyropheophorbide a in dimethylformamide solution, *Gen. Physiol. Biophys*., 2009, **28**, 70–77.
3. ANDREWS, D.L., A.A. DEMIDOV, *Resonance Energy Transfer*, Wiley, Chichester, 1999.
4. ARGUSLAB., ArgusLab (tm). Program package. Version 4.0. Planaria Software LLC, 2004.
5. AVOURIS, P., W. GELBART, M. EL-SAYED, Nonradiative electronic relaxation under collision-free conditions, *Chem. Rev*., 1977, **77**, 793–831.
6. BAUMANN, J., M.D. FAYER, Excitation transfer in disordered two-dimensional and anisotropic three-dimensional systems: effects of spatial geometry on time- resolved observables, *J. Chem. Phys*., 1986, **85**, 4087–4107.
7. BONNETT, R., Photosensitizers of the porphyrin and phthalocyanine series for photodynamic therapy, *Chem. Soc. Rev.*, 1995, **24**, 19–33.
8. DALE, R.E., R.E.J. EISINGER, Intramolecular distances determined by energy transfer dependence on orientational freedom of donor and acceptor, *Biopolymers J*. 1974, **13**, 1573–1605.
9. DAVYDOV, A.S., *Theory of Molecular Excitons*, McGraw Hill Book Company, New York, 1962.
10. DEXTER, D.L., A theory of sensitized luminescence in solids, *J. Chem. Phys*., 1953, **21**, 836–850.
11. DOLMANS, D.E., A. KADAMBI, J.S. Hill, C.A. WATERS, B.C. ROBINSON, J.P. WALKER, D. FUKUMURA, R.K. JAIN, Vascular accumulation of a novel photosensitizer, MV6401, causes selective thrombosis in tumor vessels after photodynamic therapy, *Cancer Res*., 2002, **62**, 2151–2156.
12. FAIRCLOUGH, R.H., C.R. CANTOR, The use of singlet-singlet energy transfer to study macromolecular assemblies, in *Methods in Enzymology*, New York, Academic Press, 1994.
13. FÖRSTER, T., Zwischenmolekulare Energiewanderung und Fluoreszenz, *Annalen der Physik.*, 1948, **2**, 55–75.

14. FRANZEN, J.S., P.S. MARCHETTI, D.S. FEINGOLD, Resonance energy transfer between catalytic sites of bovine liver uridine diphosphoglucose dehydrogenase, *Biochem*., 1980, **19**, 6080–6089.
15. GUILBAULT, G.G.**,** *Practical Fluorescence*. 2nd edition, Marcel Dekker, Inc., New York, 1990.
16. GUPTASARMA, P., B. RAMAN, Use of tandem cuvettes to determine whether radiative (trivial) energy transfer can contaminate steady-state measurements of fluorescence resonance energy transfer*, Anal. Biochem.,* 1995, **230**, 187–191.
17. HAAS, E., E. KATCHASLSKI-KATZIR, I.Z. STINBERG, Brownian motion of the ends of oligopeptide chains in solution as estimated by energy transfer between the chain ends, *Biopolymers*., 1978, **17**, 11–13.
18. HACKBARTH, S., V. HORNEFFER, A. WIEHE, F. HILLENKAMP, Photophysical properties of pheophorbide-a-substituted diaminobutane poly-propylene-imine dendrimer, *Chem. Phys*., 2001, **269**, 339–346.
19. KADISH, K.M., K.M. SMITH, R. GUILARD, *The Porphyrin Handbook*, Academic Press, Boston, 1999.
20. KASHA, M., Energy transfer mechanisms and the molecular exciton model for molecular aggregates, *Radiation Research*, 1963, **20**, 55–71.
21. KASHA, M., H.R. RAWLS, A.M. El-BAYOUMI, The exciton model in molecular spectroscopy, *Pure. Appl. Chem*., 1965, **11**, 371–392.
22. KAVARNOS, G. J., *Fundamentals of Photoinduced Electron Transfer*, VCH Publishers Inc, USA, 1993.
23. KESSEL, D., T. DOUGHERTY, *Porphyrin Photosensitization*, Plenum Press, New York, 1983.
24. KLEIMA, F.J., E. HOFMANN, B. GOBETS, I.H.M. VAN STOKKUM, R. VAN GRONDELLE, K. DIEDERICHS, H. Van AMERONGEN, Förster excitation energy transfer in peridinin-chlorophyll-*a*-protein, *Biophys. J*., 2000, **78**, 344–535.
25. LAKOWICS, J.R., *Principles of Fluorescence Spectroscopy*, 1st edn, Plenum Press, New York, 1983.
26. LIN S.H., Isotope effect, energy gap law and temperature effect in resonance energy transfer, *Mol. Phys*., 1971, **21**, 853–863.
27. LIN, S.H., W.Z. XIAO, Generalized Förster Dexter theory of photoinduced intramolecular energy transfer, *Phys. Rev*., 1993, **47**, 3698–3706.
28. MARQUARDT, D.W., Analgorithm for least-squares estimation of nonlinear parameters, *SIAM J. Soc. Ind. Appl. Math*., 1963, **11**, 431–441.
29. MATROULE, J.Y., C.M. CARTHY, D.J. GRANVILLE, O. JOLOIS, D.W.C. HUNT, J. PIETTE, Mechanism of colon cancer cell apoptosis mediated by pyropheophorbide-a methyl ester photosensitization, *Oncogene*, 2001, **20**, 4070–4084.
30. MATROULE, J.Y., G. BONIZZI, P. MORLIE`, N. PAILLOUS, R. SANTS, V. BOURS, J. PIETTE, Pyropheophorbide-a methyl ester-mediated photosensitization activates transcription factor NF-kB through the interleukin-1 receptor-dependent signaling pathway, *J. Biol. Chem*., 1999, 274, 2988–3000.
31. McRAE, E.G., M. KASHA, *Physical Processes in Radiation Biology*, Academic Press, New York, 1964.
32. MITRA, R.D., C.M. SILVA, D.C. YOUVAN, Fluorescence resonance energy transfer between blue-emitting and red-shifted excitation derivatives of the green fluorescent protein, *Gene*., 1996, **173**, 13–17.
33. MORRIS, R.L., K. AZIZUDDIN, M. LAM, J. BERLIN, A.L. NIEMINEN, M.E. KENNEY, A.C.S. SAMIA, C. BURDA, N.L. OLEINICK, Fluorescence resonance energy transfer reveals a binding site of a photosensitizer for photodynamic therapy, *Cancer. Res*., 2003, **63**, 5194–5197.
34. PANDEY, R.K., A.B. SUMLIN, S. CONSTANTINE, M. AOUDIA, W.R. POTTER, D.A. BELLINIER, B.W. HENDERSON, M.A. RODGERS, K.M. SMITH, T.J. DOUGHETRY, Synthesis, photophysical properties, and photodynamic efficacy of alkyl ether analogs of chlorophyll-a derivatives, *Photochem. Photobiol.,* 1996*,* **52**, 644–651.

35. PARKER, C.A., *Photoluminescence of Solutions*., Elsevier, New York, 1968.
36. POLKING, J., A. BOGGESS, D. ARNOLD, *Differential Equations*, 2nd edition, Prentice Hall, USA, 2005.
37. ROBINSON, G.W., R.P. FROSCH, Theory of electronic energy relaxation in the solid phase, *J. Physical. Chem*., 1962, **37**, 1962–1973.
38. RUBIO, N., F. PRAT, N. BOU, J.I. BORRELL, J. TEIXIDÓ, Á. VILLANUEVA, Á. JU ARRANZ, M. CAŃETE, J.C. STOCKERTB, S. NONELLI. A comparison between the photophysical and photosensitizing properties of tetraphenyl porphycenes and porphyrins, *New. J. Chem*., 2005, **29**, 378–384.
39. RUECKMANN, I., A. ZEUG, R. HERTER, B. ROEDER, On the influence of higher excited states on the ISC quantum yield of octa-a-alkyloxy–substituted Zn-phthalocyanine molecules studied by nonlinear absorption, *Photochem. Photobiol*., 1997, **66**, 576–584.
40. RUECKMANN, I., A. ZEUG, T. Von FEILITZSCH, Orientational relaxation of pheophorbide-a molecules in the ground and in the first excited state measured by transient dichroism spectroscopy, *Opt. Com*., 1999, **170**, 361–372.
41. SCHWEITZER C., R. SCHMIDT, Physical mechanisms of generation and deactivation of singlet oxygen, *Chem. Rev.*, 2003, **103**, 1685–1757.
42. SIMPSON, W.T., D.L. PETERSON, Coupling strength for resonance force transfer of electronic energy in Van der Waals solids, *J. Chem. Phys*., 1957, **26**, 588–593.
43. SPEISER S., Photophysics and mechanisms of intramolecular electronic energy transfer in bichromophoric systems: solution and supersonic jet studies, *Chem. Rev*., 1996, **96**, 1953–1976.
44. SPIKER, J.D., J.C. BOMMER, *Chlorophyll and Related Pigments as Photosensitizers in Biology and Medicine*, *in Chlorophyll*. H, Scheer, ed. CRC Press, Florida, 1991.
45. STRYER, L., Fluorescence energy transfer as a ruler, *Annu. Rev. Biochem.*, 1978, 47, 819–846.
46. SUN, X.; W.N. LEUNG, Photodynamic therapy with pyropheophorbide-a methyl ester in human lung carcinoma cancer cell: efficacy, localization and apoptosis, *Photochem. Photobiol.*, 2002, **75**, 644–651.
47. TURRO, N.J., *Modern Molecular Photochemistry*, Benjamin/Cummings, Menlo Park, CA, 1987.
48. VALEUR, B., *Molecular Florescence: Principles and Applications*, Wiley-VCH Verlag GmbH, Weinheim, Germany, 2001.
49. WEHRY, E.L., *Modern Fluorescence Spectroscopy*, Plenum Press, New York, 1976.
50. WU, P., L. BRAND, Resonance energy transfer: methods and applications, *Anal. Biochem*., 1996, **218**, 1–13.
51. YEOW, E.K.L., K.P. GHIGGINO, J.N.H. REEK, M.J. CROSSLEY, A.W. BOSMAN, A.P. H.J. SCHENNING, E.W. MEIJER, The dynamics of electronic energy transfer in novel multiporphyrin functionalized dendrimers: A time-resolved fluorescence anisotropy study, *J. Phys. Chem. B*., 2000, **104**, 2596–2606.
52. YOKOTA, M., O. TANIMOTO, Effects of diffusion on energy transfer by resonance, *J. Phys. Soc. Jpn*., 1967, **22**, 779–784.